LA-UR-18-27512

Approved for public release; distribution is unlimited.

Title:	Virtual characterization: perspectives
Author(s):	Capolungo, Laurent
Intended for:	Scientific presentation/discussion to be given to the LEM3 laboratory in Metz, France. The talk is planned on July 26th.
Issued:	2018-08-07

Virtual characterization: perspectives

L. Capolungo

Acknowledgement: BES E401

Outline

- Integrated modeling: discrete continuous model embedded in a Fast Fourier Transform mechanical solver
- Virtual characterization
  - Connecting with Xray Diffraction
  - Connection with TEM

Integrated multi-scale modeling: approach and prospects

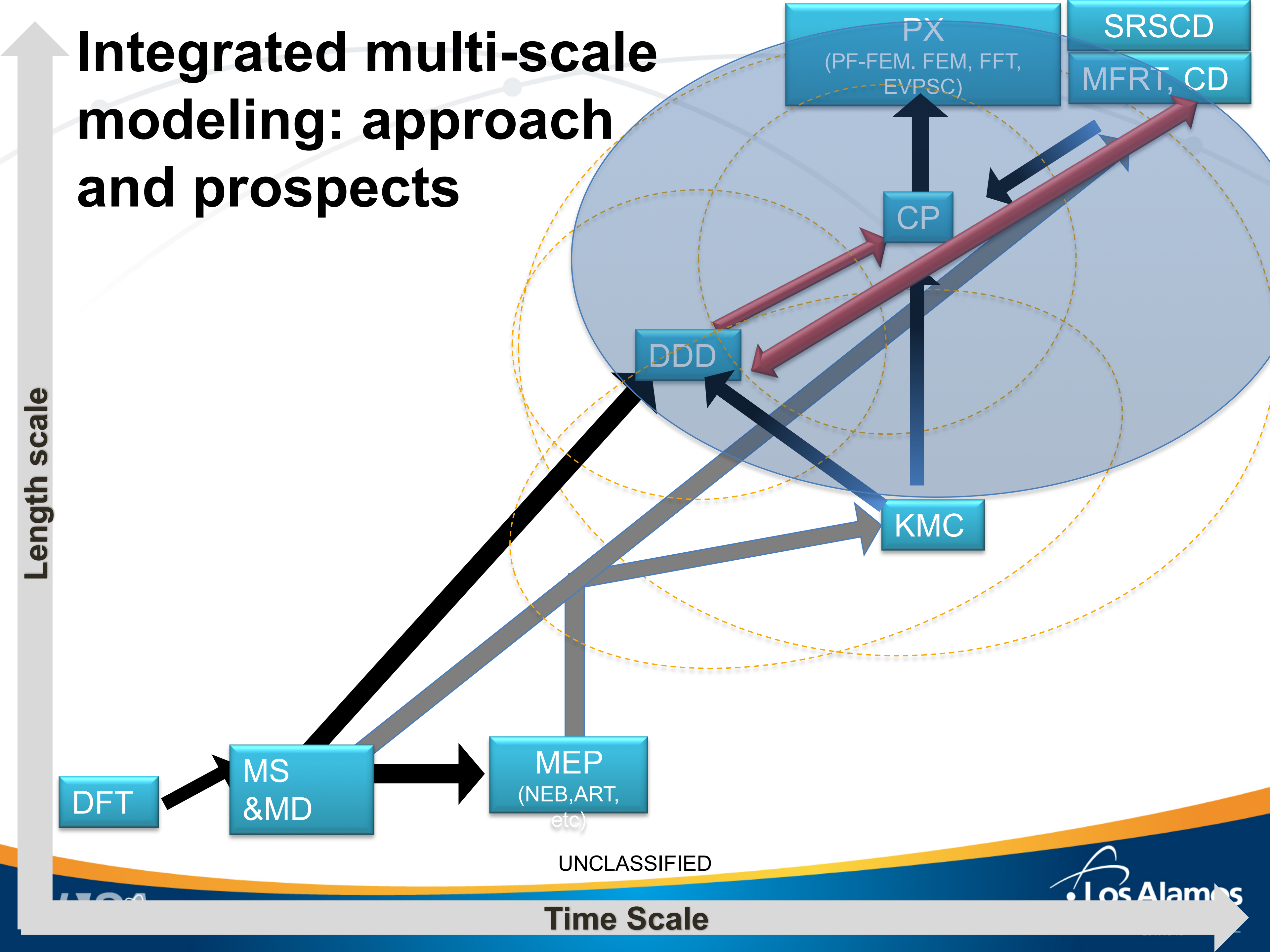

UNCLASSIFIED

A FFT based Formulation:

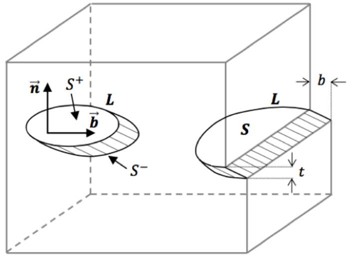

$$\epsilon^p_{ij}(\vec{\boldsymbol{x}}) = -\frac{1}{2}\left(b_i n_j + b_j n_i\right)\delta(\vec{\boldsymbol{S}} - \vec{\boldsymbol{x}})$$

The plastic strain due to dislocation motion is treated as an eigenstrain

$$\begin{cases} \boldsymbol{\sigma}(\vec{\boldsymbol{x}}) = \boldsymbol{C}(\vec{\boldsymbol{x}}) : (\boldsymbol{\epsilon}(\vec{\boldsymbol{x}}) - \boldsymbol{\epsilon}^p(\vec{\boldsymbol{x}})) \\ \mathbf{div}\ \boldsymbol{\sigma}(\vec{\boldsymbol{x}}) = \vec{\mathbf{0}} \end{cases} \qquad \forall \vec{\boldsymbol{x}} \in V$$

The system is equilibrated and constitutively related

The polarization tensor can include SFTS, Plasticity

$$\boldsymbol{\sigma}(\vec{\boldsymbol{x}}) = \boldsymbol{C}^0 : \boldsymbol{\epsilon}(\vec{\boldsymbol{x}}) + \boldsymbol{\tau}(\vec{\boldsymbol{x}})$$
$$\boldsymbol{\tau}(\vec{\boldsymbol{x}}) = \boldsymbol{\delta C}(\vec{\boldsymbol{x}}) : \boldsymbol{\epsilon}(\vec{\boldsymbol{x}}) - \boldsymbol{C}(\vec{\boldsymbol{x}}) : \boldsymbol{\epsilon}^p(\vec{\boldsymbol{x}})$$
$$\boldsymbol{\delta C}(\vec{\boldsymbol{x}}) = \boldsymbol{C}(\vec{\boldsymbol{x}}) - \boldsymbol{C}^0$$

One can rewrite the constitutive relationship

$$C^0_{ijkl} u_{k,lj}(\vec{\boldsymbol{x}}) + \tau_{ij,j}(\vec{\boldsymbol{x}}) = 0 \qquad \forall \vec{\boldsymbol{x}} \in V$$

One obtains the Lippmann Schwinger equation

$$\begin{aligned} \widehat{\boldsymbol{\epsilon}}(\vec{\boldsymbol{\xi}}) &= -\widehat{\boldsymbol{\Gamma}}^0(\vec{\boldsymbol{\xi}}) : \widehat{\boldsymbol{\tau}}(\vec{\boldsymbol{\xi}}) & \forall \vec{\boldsymbol{\xi}} \neq \vec{\mathbf{0}}, \\ &= -\widehat{\boldsymbol{\Gamma}}^0(\vec{\boldsymbol{\xi}}) : \widehat{\boldsymbol{\delta C} : \boldsymbol{\epsilon}}(\vec{\boldsymbol{\xi}}) + \widehat{\boldsymbol{\Gamma}}^0(\vec{\boldsymbol{\xi}}) : \widehat{\boldsymbol{C} : \boldsymbol{\epsilon}^p}(\vec{\boldsymbol{\xi}}) & \widehat{\boldsymbol{\epsilon}}(\vec{\mathbf{0}}) = \boldsymbol{E} \end{aligned}$$

Which is solved in Fourier space

Bertin et al. MSMSE 2015, Bertin et al. , Lemarchand et al.1998

Concurrent multi-scale

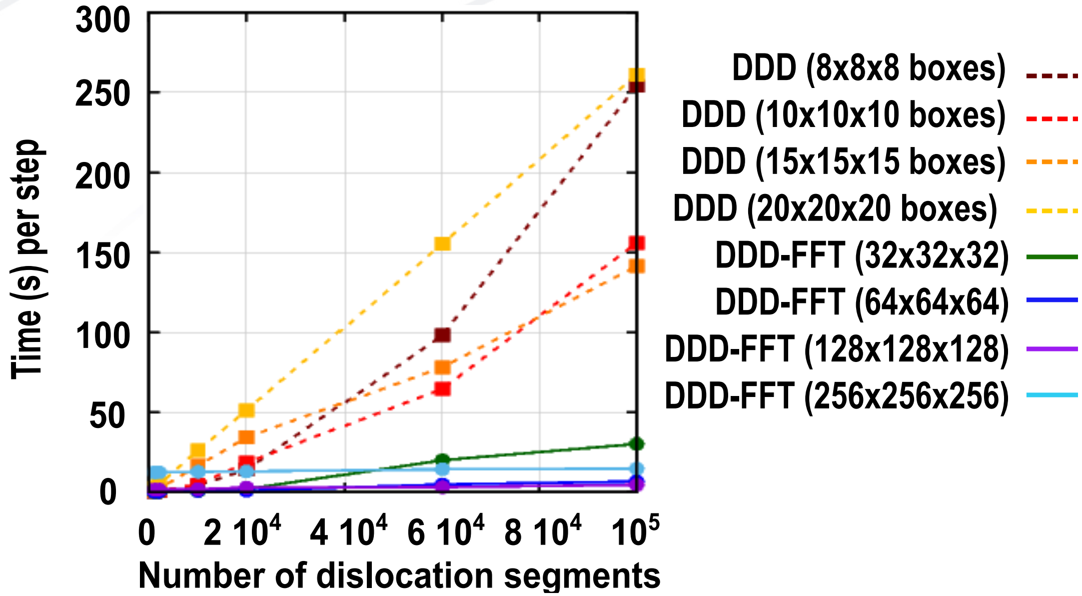

A conjugate gradient algorithm allows for the simulations of plasticity in heterogeneous media

Convergence is reached even with 10^5 stiffness contrasts

G_1 (Material 1)	G_2 (Material 2)
26.175 GPa	261.75 GPa

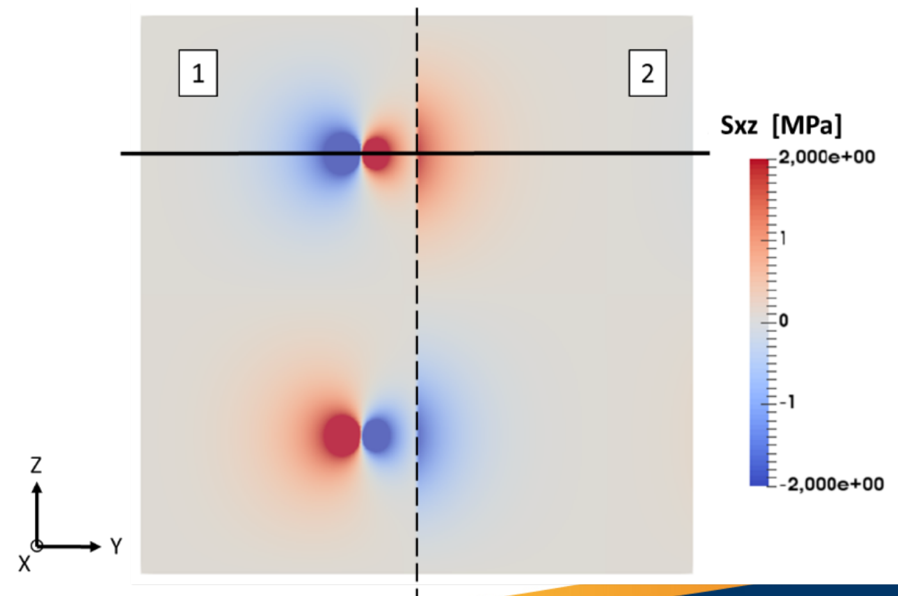

The FFT based DDD tool allows for a treatment of anisotropic elasticity

Highly computationally efficient (i.e. runs on a laptop with GPU card)

Bertin et al. MSMSE 2015, Bertin et al.

The FFT algorithm accelerates the computation of forces on segments.

→Computational times are not very sensitive to dislocation content.

- → Heterogeneous problems can be solved (PX, SFTS)
- → Anisotropic problems have no extra cost

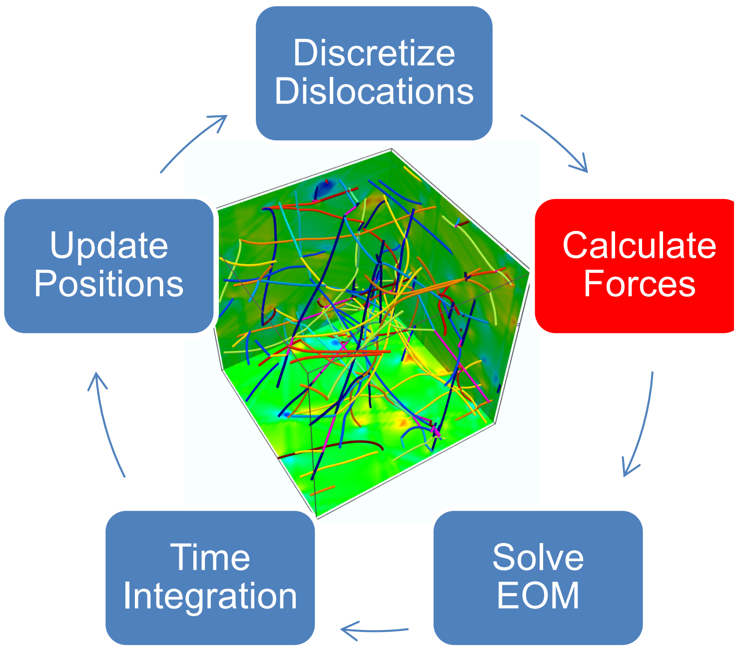

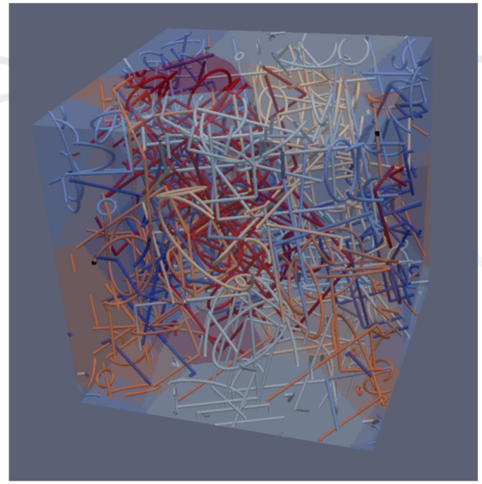

Polycrystal simulations to large densities

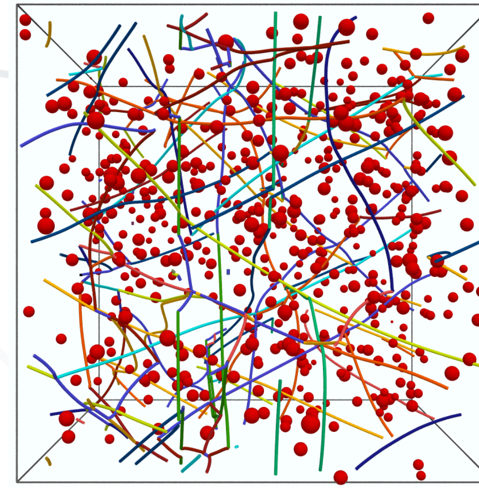

Coupling between mechanics and chemistry (vacancy accumulation during irradiation)

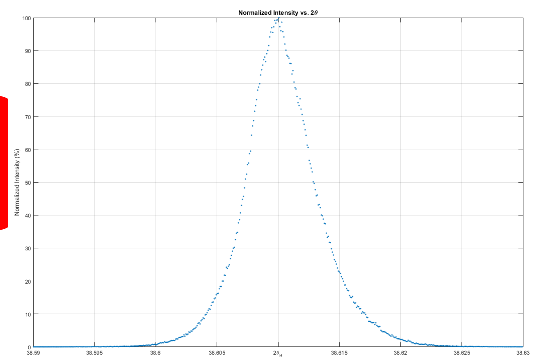

On the fly diffraction peak calculations

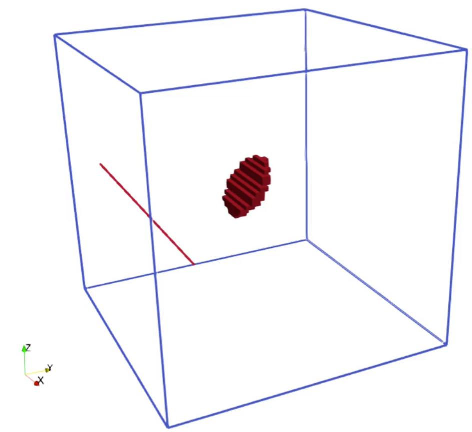

Internal stress assisted cross-slip in Al-Cu

UNCLASSIFIED

Revisiting the grain size effect

- Multiple copper polycrystalline samples were pulled in tension at a strain rate 10^5 s^{-1}
- 64x64x64 point Fourier grid
- Grain sizes were varied from ~150 to 500 nm
- No grain boundary transmission

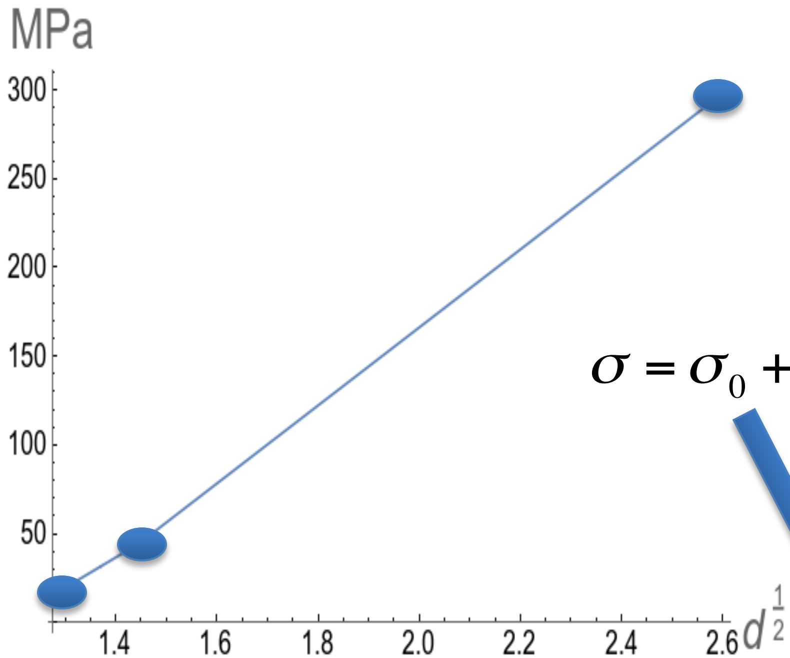

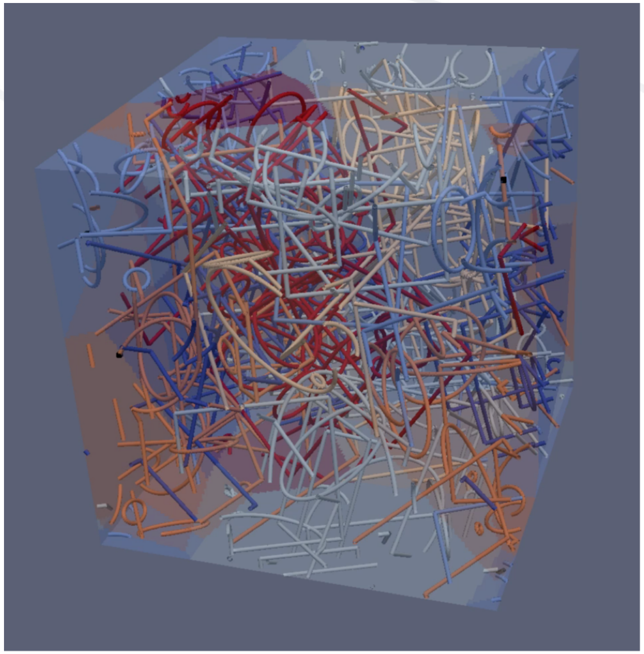

Grain boundaries are taken as impenetrable obstacles

$$\sigma = \sigma_0 + \frac{k}{\sqrt{d}}$$

Predicted : 0.148 MPa.m$^{1/2}$
Reported: 0.14 Mpa.m$^{1/2}$

Predicted : 14 MPa
Reported: 20 MPa

UNCLASSIFIED

Hansen et al., Scripta Mat 2004

Outline

- Integrated modeling: discrete continuous model embedded in a Fast Fourier Transform mechanical solver
- Virtual characterization
  - Connection with TEM
  - Connecting with Xray Diffraction

Line Profile Analysis: Wilkens approach

Scattering intensity

$$I(\vec{\kappa}) = C\sum_{j,l=2}^{N} \exp\left(i\vec{\kappa}\left(\vec{R}_j - \vec{R}_l\right)\right)$$

$$I(\vec{s}) = \exp(i\pi\vec{s}\vec{n})\frac{C}{V}\int dn^3 \int dr^3 \exp\left(2\pi i\vec{g}\left(u(\vec{r}+\vec{n}/2)-u(\vec{r}-\vec{n}/2)\right)\right)$$

Scattering intensity is proportional to the Fourier Transform of

$$A(\vec{n}) = \frac{1}{V}\int dr^3 \exp\left(2\pi i\vec{g}\left(u(\vec{r}+\vec{n}/2)-u(\vec{r}-\vec{n}/2)\right)\right)$$

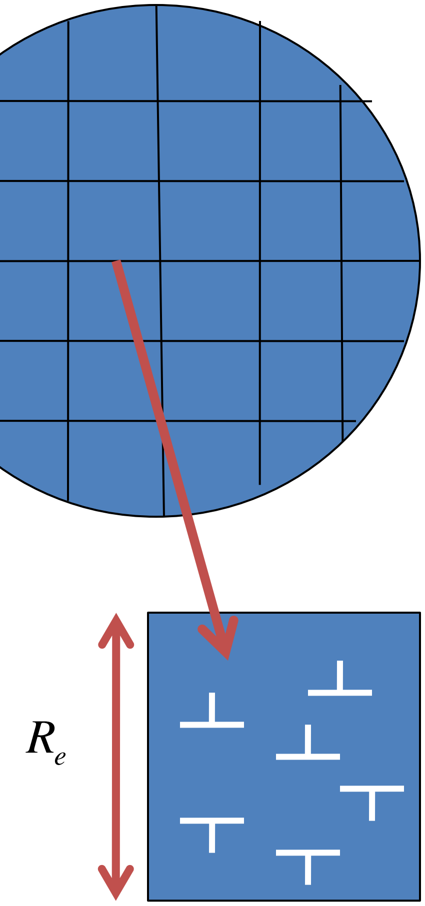

Warren Averbach relation

$$A(\vec{n}) = \exp\left(-2\pi^2 n^2 g^2 < \varepsilon_{g,n}^2 >\right)$$

Wilkens

$$< \varepsilon_{g,n}^2 > = -\left(\frac{b}{2\pi}\right)^2 \pi\rho f(\eta)$$

Asymmetric peaks in work of Groma et al.
Effect of dislocation contrasts Ungar et al.

$$\eta = \frac{1}{2}\exp(-1/4)\, L/R_e$$

Line Profile Analysis: Wilkens approach

Restrictedly random distributions:

The crystal can be subdivided in subvolumes of equal size in which:

-All have same dislocation densities.
-Which have a null net dislocation polarity.
-All dislocations are infinitely long straight and parallel
-Within each volume the dislocation distribution is random

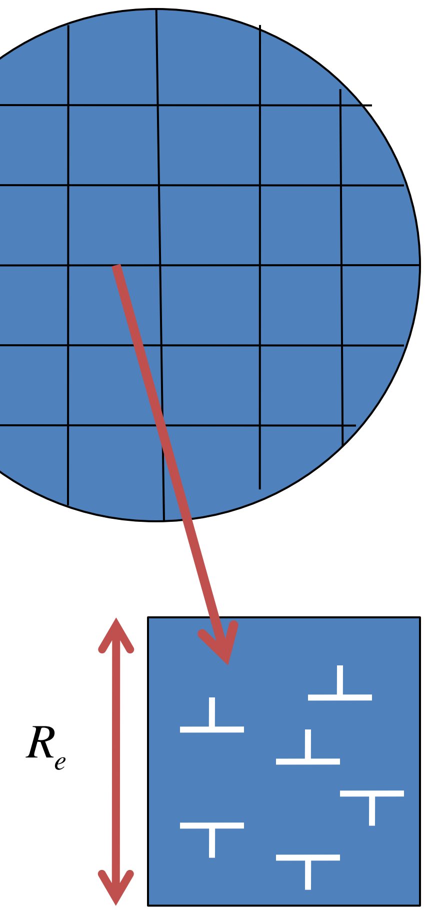

Warren Averbach relation $$A(\vec{n}) = \exp\left(-2\pi^2 n^2 g^2 < \varepsilon_{g,n}^2 >\right)$$

Wilkens $$< \varepsilon_{g,n}^2 >= -\left(\frac{b}{2\pi}\right)^2 \pi\rho f(\eta)$$

Asymmetric peaks in work of Groma et al.
Effect of dislocation contrasts Ungar et al.

$$\eta = \frac{1}{2}\exp(-1/4)\, L/R_e$$

Balogh et al. 2012

Peak profile construction

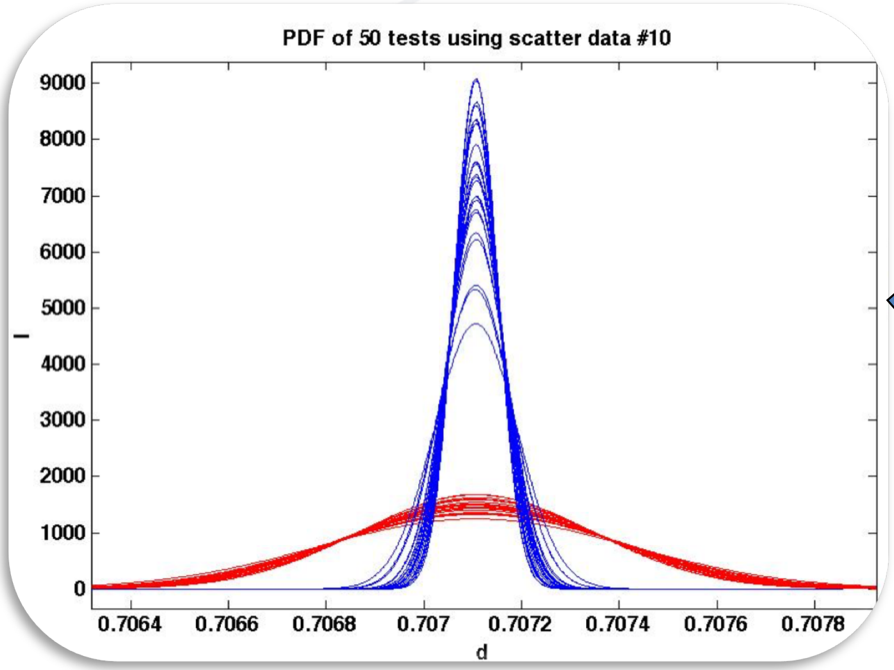

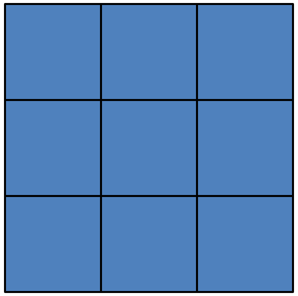

To create representative peaks, several (i.e. 8-20) dislocation structures with same densities are generated.

Accuracy of line profile analysis as a function of dislocation density: relatively homogeneous distributions

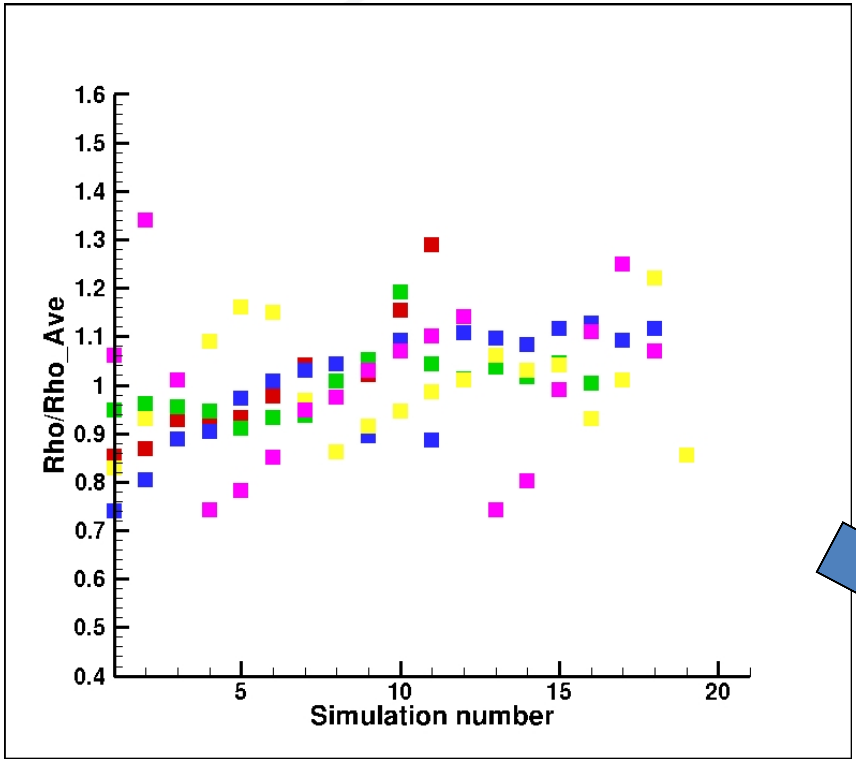

Sample relative densities

1.e12	red
2.5e12	green
5.e12	blue
5e13	yellow
1e14	magenta

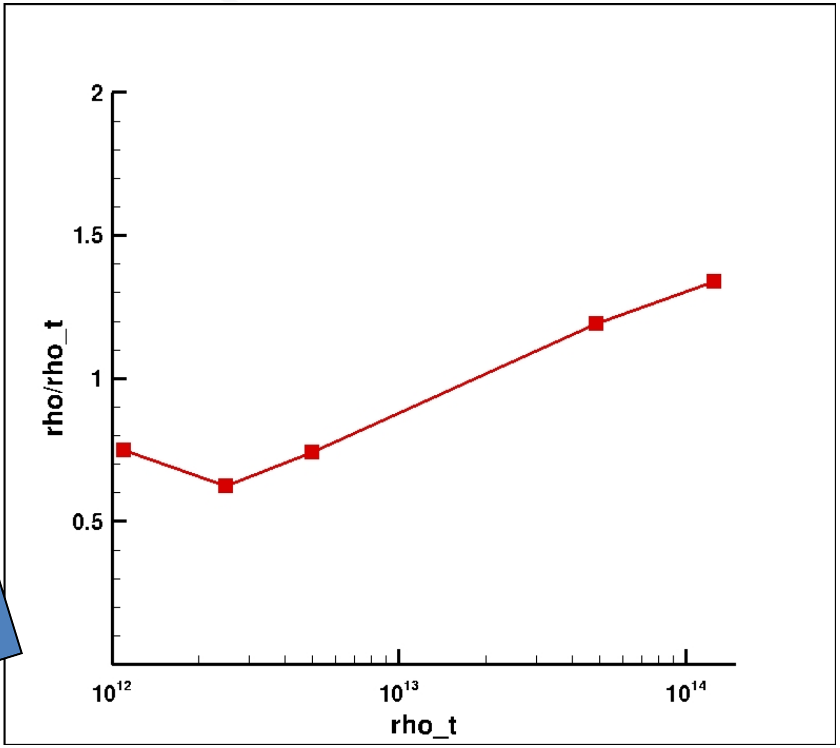

Evolution Ratio of density predicted from line profile analysis over density produced by dislocation dynamics

Balogh et al. Acta Mater 2012

Accuracy of line profile analysis as a function of dislocation density: Inhomogeneous distributions

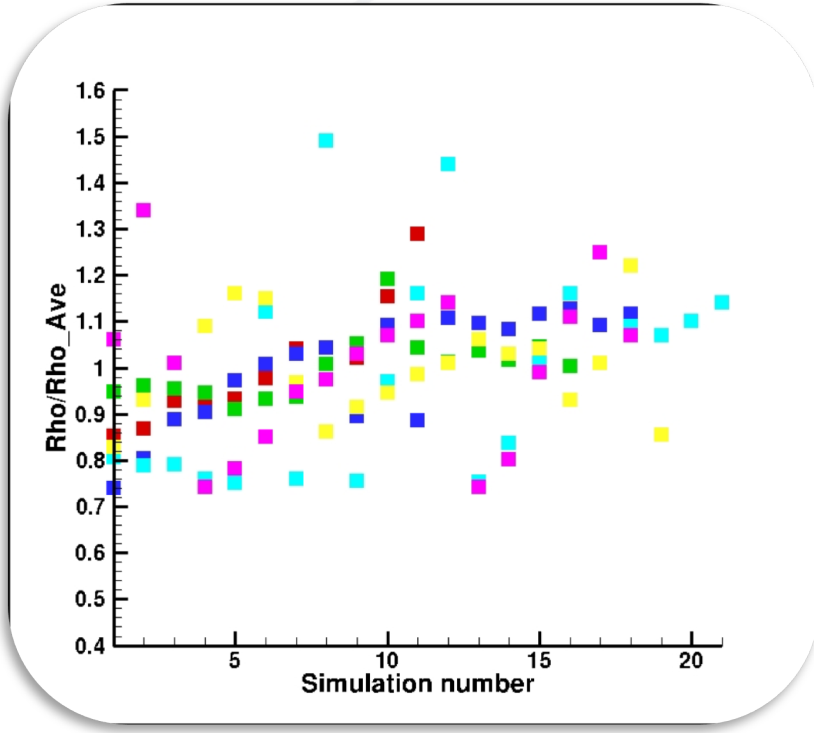

Sample relative densities

1.e12
2.5e12
5.e12
1.e13
5e13
1e14

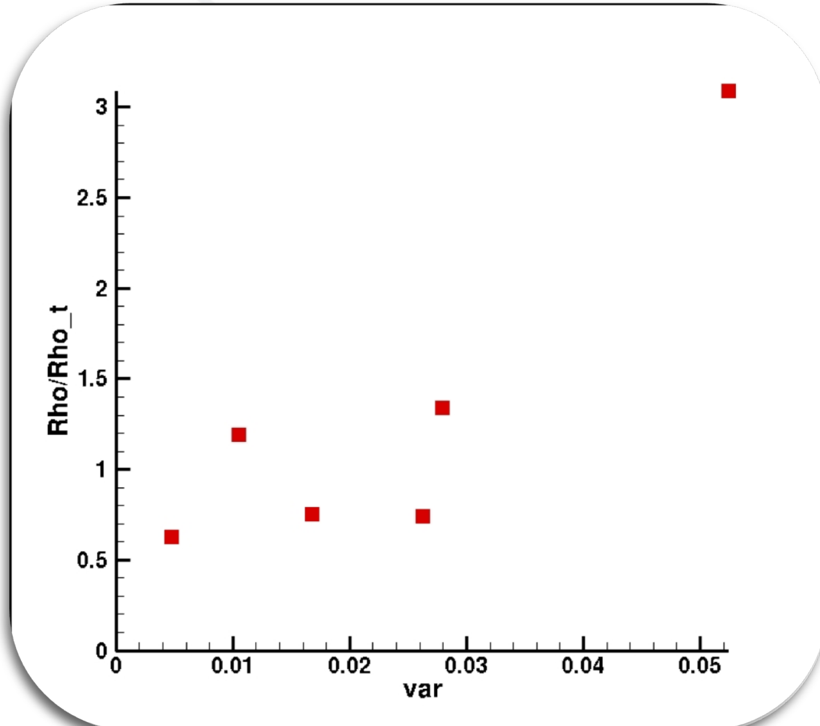

A modest departure from homogeneous distribution significantly increases the error of line profile analysis

Balogh et al. Acta Mater 2012

Outline

- Integrated modeling: discrete continuous model embedded in a Fast Fourier Transform mechanical solver
- Virtual characterization
  - Connecting with Xray Diffraction
  - Connection with TEM

Numerical FIB

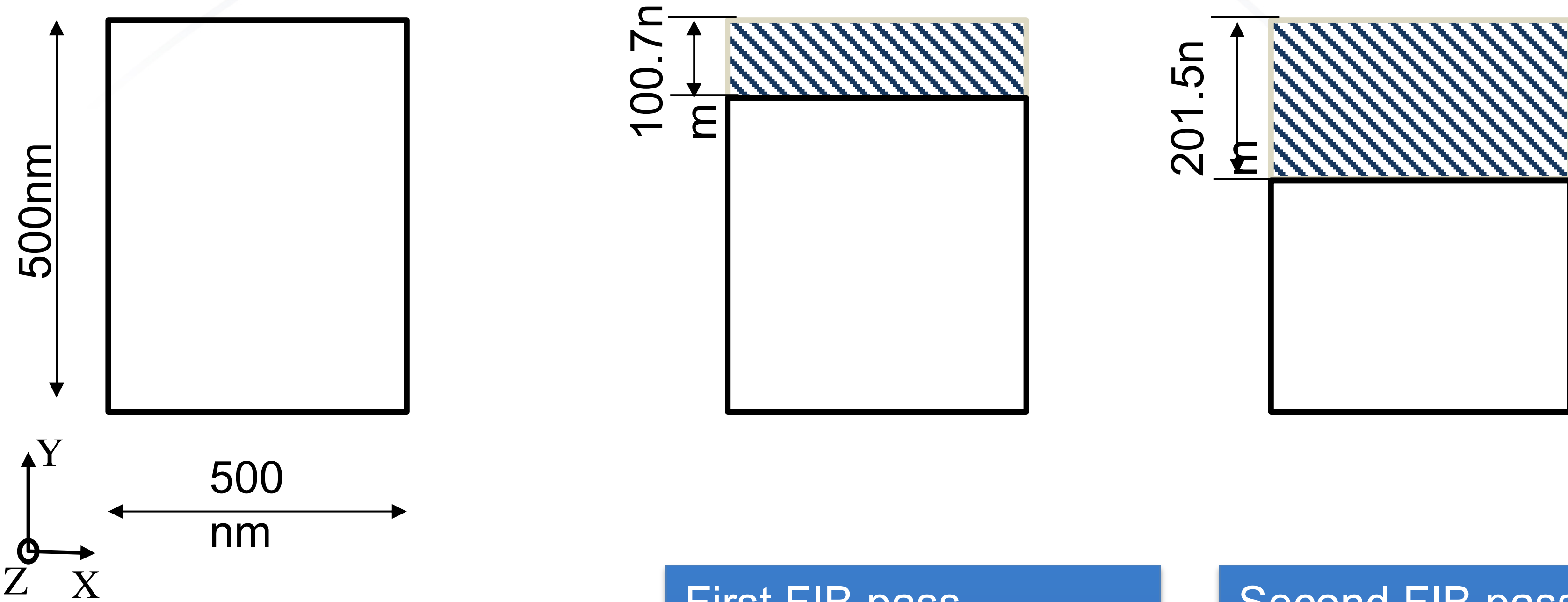

Initial microstructure containing a relaxed dislocation configuration

First FIB pass (~100nm) followed by relaxation.
Dislocations can exit the system

Second FIB pass (~100nm) followed by relaxation.
Dislocations can exit the system

Virtual dislocation microstructure

PBC$_{xyz}$

$\Sigma_{ave}=0$

- Relaxation under local dislocation stress field

✓ 64x64x64 FFT grid
✓ Sim. Box=500nm
✓ Heterogeneous elasticity
✓ Mg$_{@273K}$

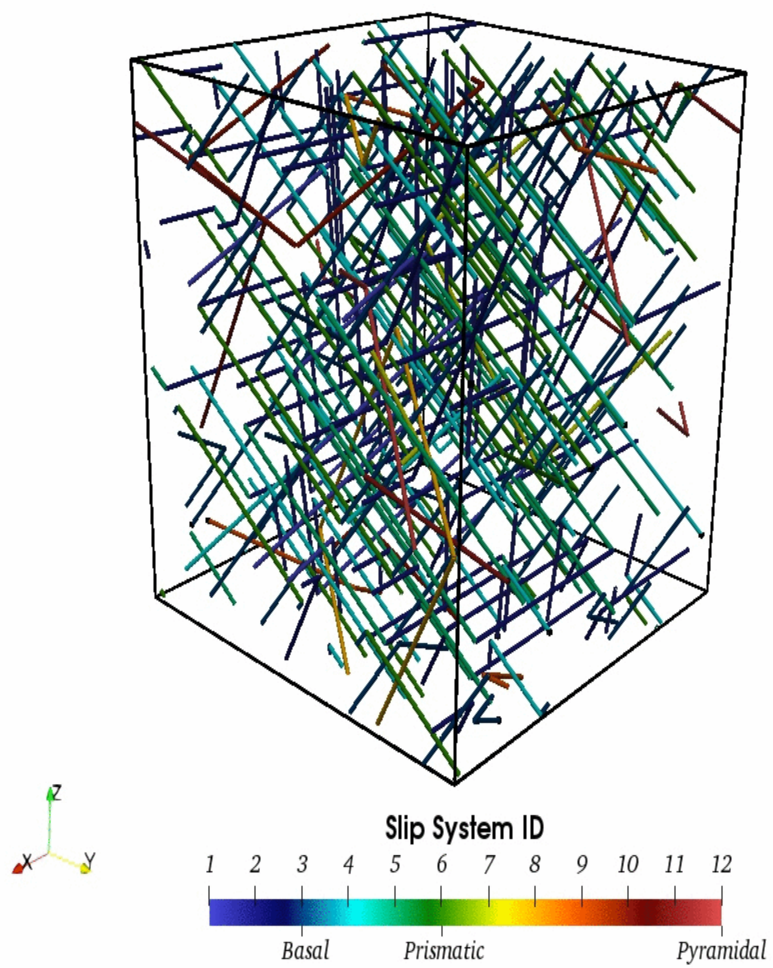

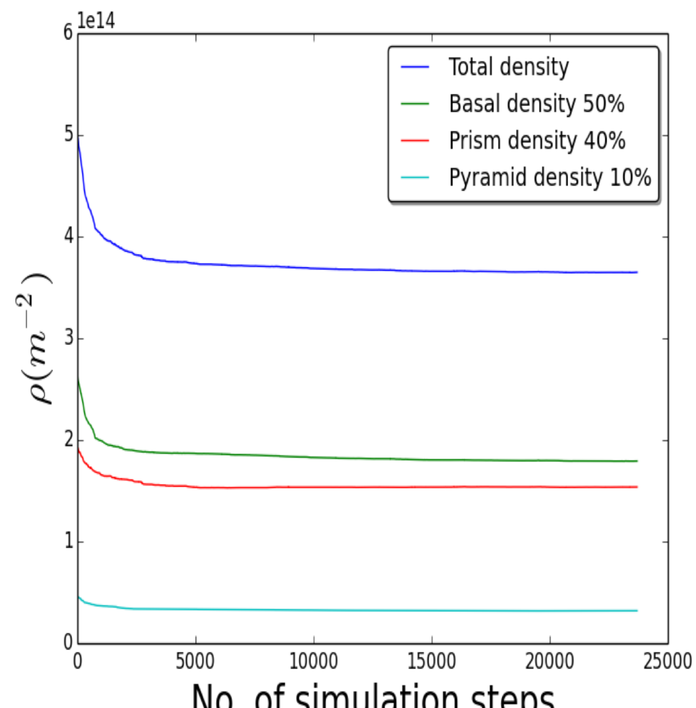

Setup for Modelling of FIB milling

$\Sigma_{ave}=0$

$PBC_{xy}+F$
S_z

- ✓ 4 consecutive milling passes
- ✓ Different virtual dislocation microstructure

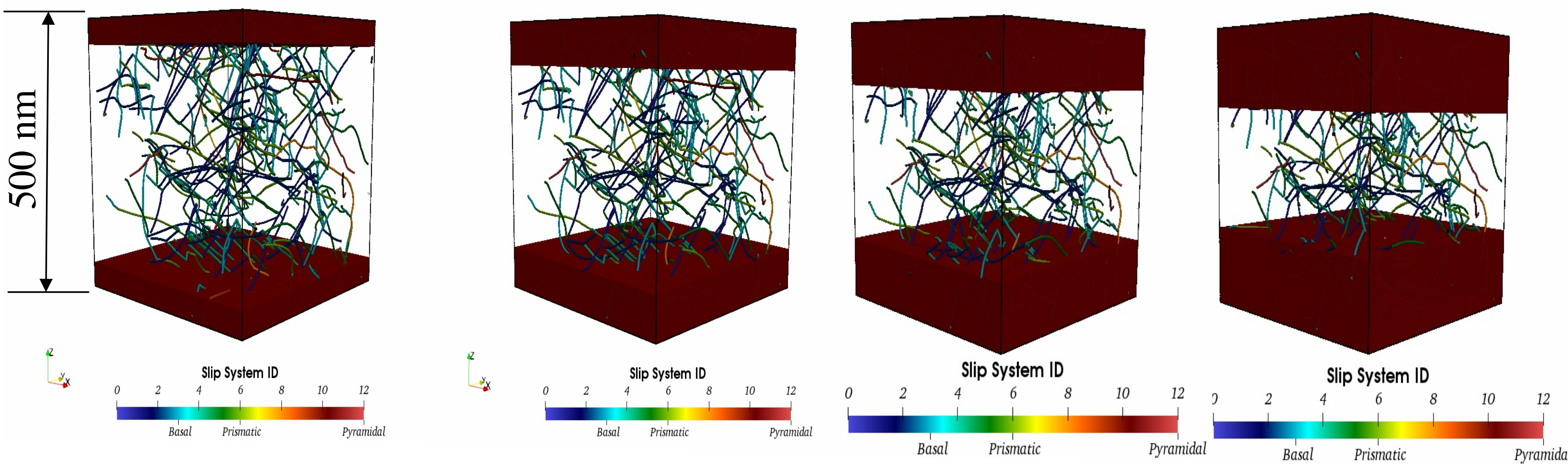

- ➢ PBC = Periodic boundary condition
- ➢ FS = Free surface

279. nm

FIB milling Pass [01-04] – Total dislocation density

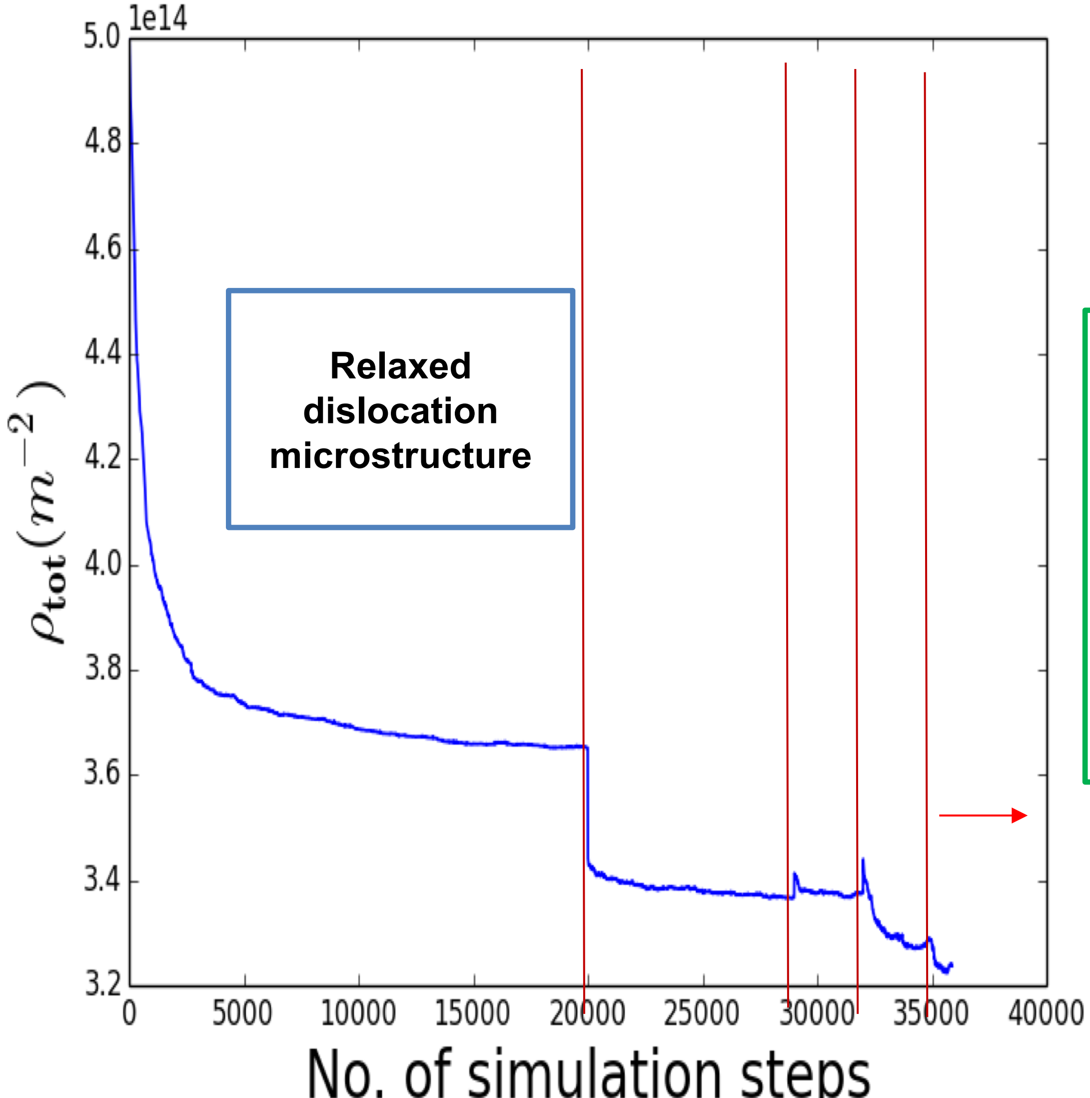

Total dislocation density decreases by ~15.6 %

FIB milling Pass– Dislocation density on each slip system

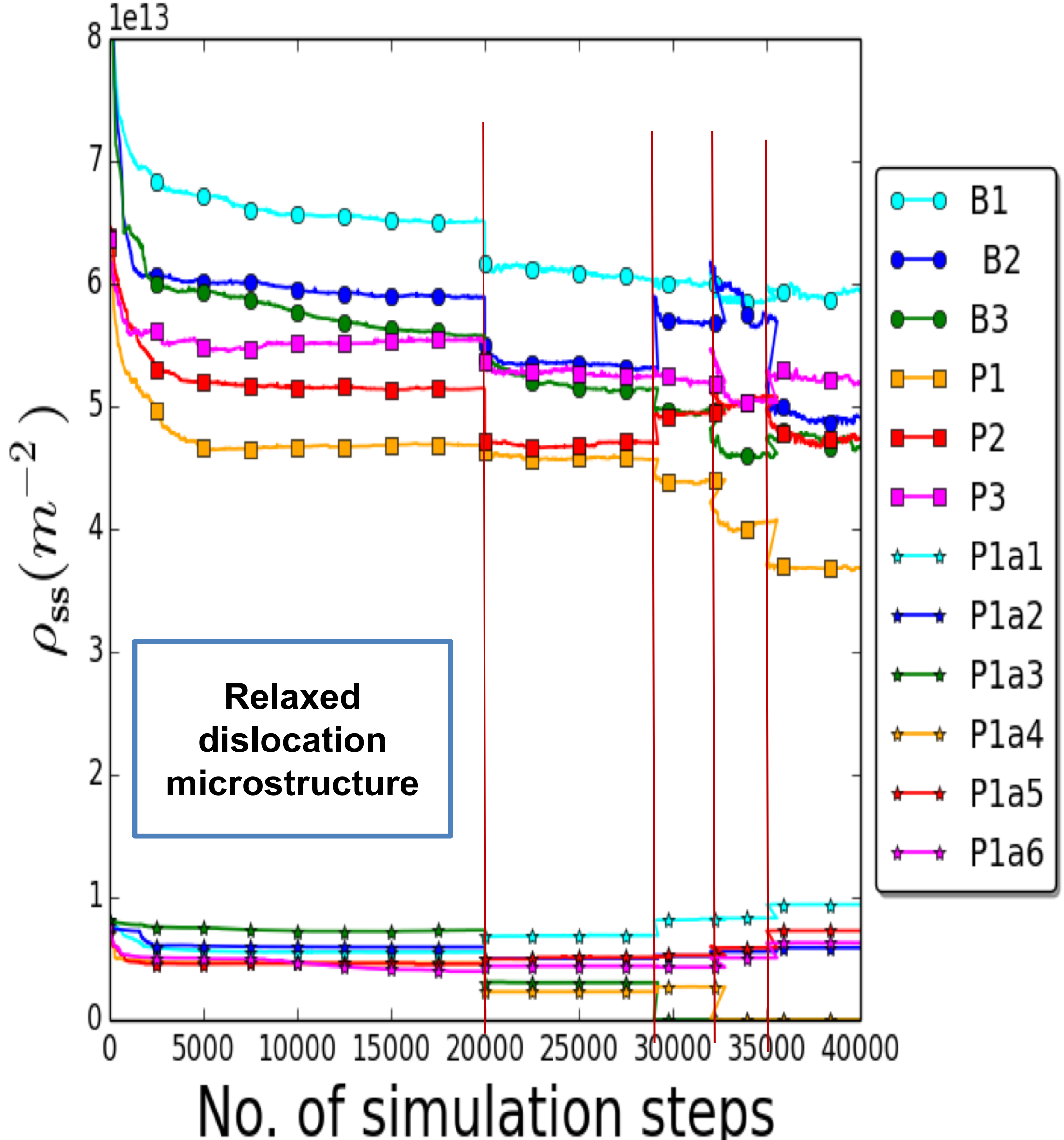

Changes in slip system activity (Eg: B2 and P3)

FIB milling Pass [01-04] – Total junction density and junction length

Relaxed dislocation microstructure

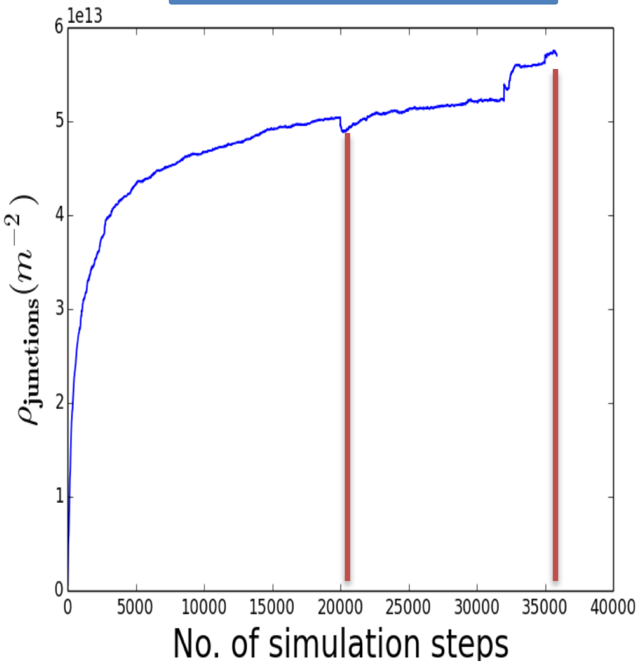

~16.3 % increase in total junction density

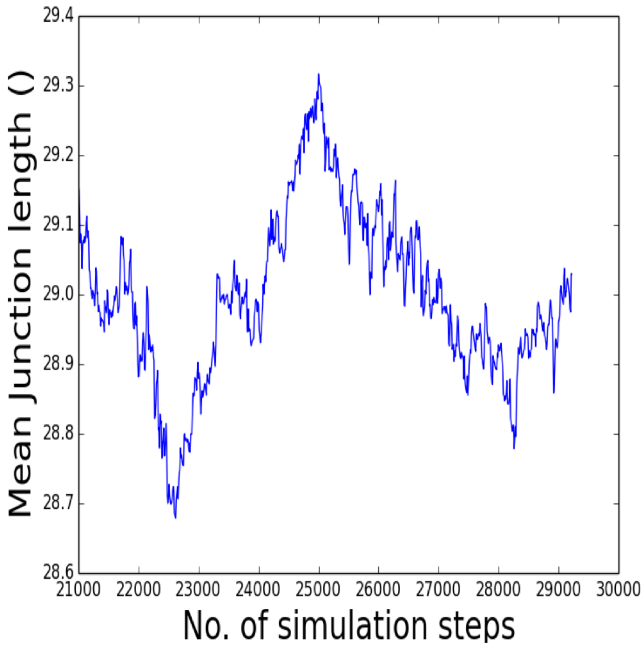

Stress relaxation due to FIB (S23)

No FIB

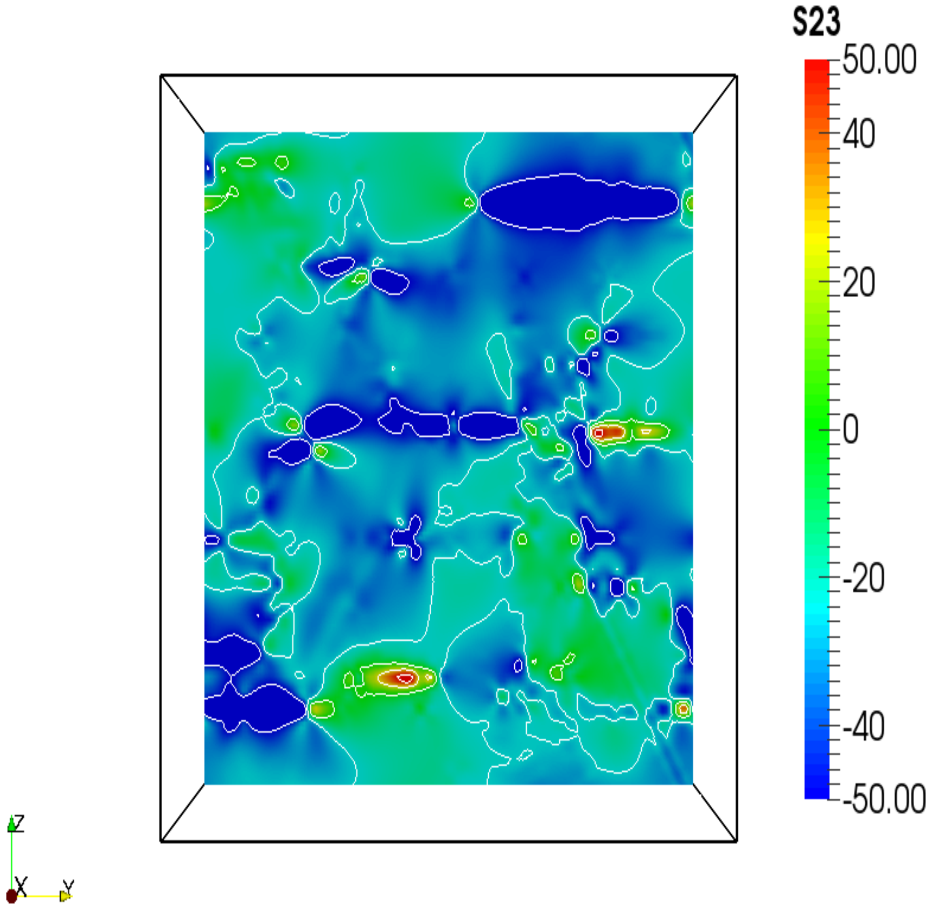

FIB

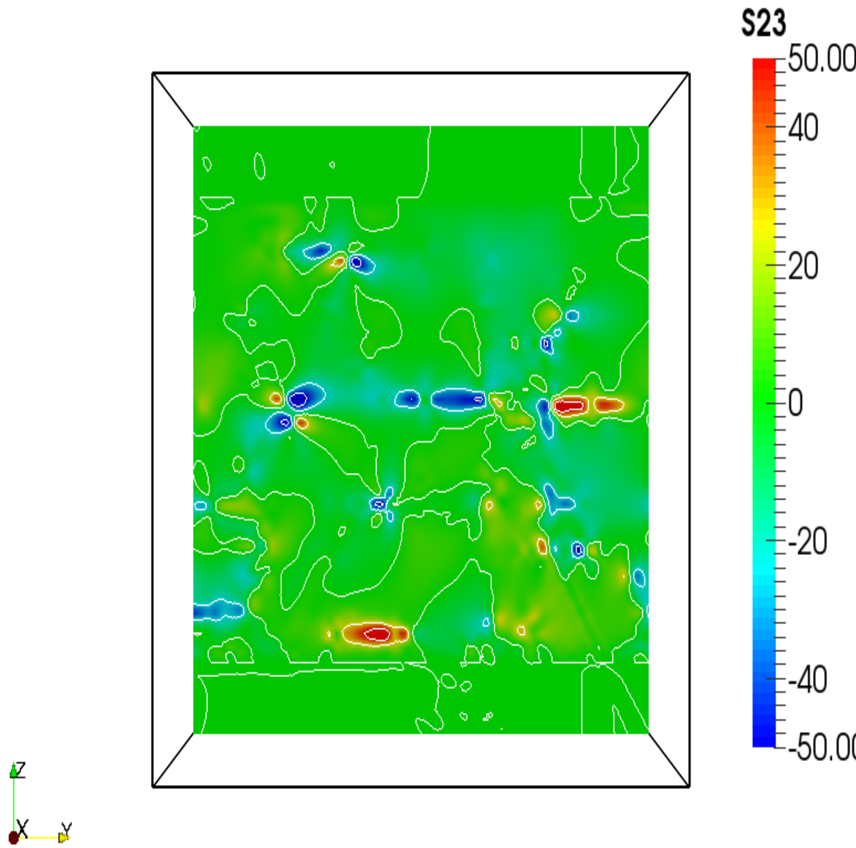

Integrated multi-scale modeling: approach and prospects